International Journal of Geo-Information

MDPI

Article

Identification of Typhoon-Vulnerable Areas and Countermeasures in High-Density Coastal Cities: The Case of Macau

Ziyi Chen [1,*], Long Zhou [1], Wenrui Li [1] and Binglin Martin Tang [2]

[1] Faculty of Innovation and Design, City University of Macau, Macau SAR, China; lzhou@cityu.edu.mo (L.Z.); u22092120087@cityu.edu.mo (W.L.)
[2] Faculty of International Tourism and Management, City University of Macau, Macau SAR, China; t22092110057@cityu.edu.mo
* Correspondence: u22092120211@cityu.edu.mo; Tel.: +853-63801059

Abstract: Typhoons are extremely severe weather events which seriously threaten the safety of people's lives and properties. Therefore, identifying and controlling typhoon disaster hazards have become important research topics. The spatial–temporal characteristics of typhoons are analysed using the typhoon disaster data in Macau from 2000 to 2020. Computational fluid dynamics (CFD) numerical simulation is adopted to understand the 3D urban wind environment. Moreover, the 'exposure, sensitivity and adaptation' evaluation model is applied to construct the study framework. To calculate urban disaster vulnerability, the Create Fishnet tool is used to divide the city of Macau into 470 grids. The principal component analysis method is used to reveal the factors that significantly affect the typhoon's vulnerable areas. Result shows that 31.27% of grids are severely vulnerable. In addition, six principal components are identified, including indicators such as population density, building area ratio, mean elevation and wind speed. This study verifies the feasibility of wind speed data obtained by CFD in the typhoon evaluation model. Moreover, it provides a reliable reference guide for future urban microlevel studies.

Keywords: high density; 3D scale; urban spatial layout; vulnerability assessment

check for updates

Citation: Chen, Z.; Zhou, L.; Li, W.; Tang, B.M. Identification of Typhoon-Vulnerable Areas and Countermeasures in High-Density Coastal Cities: The Case of Macau. *ISPRS Int. J. Geo-Inf.* **2024**, *13*, 205. https://doi.org/10.3390/ijgi13060205

Academic Editors: Godwin Yeboah and Wolfgang Kainz

Received: 24 March 2024
Revised: 4 June 2024
Accepted: 12 June 2024
Published: 17 June 2024

Copyright: © 2024 by the authors. Licensee MDPI, Basel, Switzerland. This article is an open access article distributed under the terms and conditions of the Creative Commons Attribution (CC BY) license (https://creativecommons.org/licenses/by/4.0/).

1. Introduction

Extreme weather events threaten the sustainability of coastal cities. Typhoons are one of the most important extreme weather scenarios in coastal communities [1,2]. Similar to hurricanes, typhoons are cyclones that primarily affect the western Pacific coast. They also considerably threaten personal safety and urban construction [2]. Along with the global trend of rising urban populations, low-elevation coastal cities are at substantial risk when facing typhoon disasters currently [1]. The cumulative economic damage caused by Cyclone Amphan in 2020 is as high as USD 13.6 billion [3]. Furthermore, the major contributing areas of human casualties and economic losses are the vulnerable areas of coastal cities [4].

Therefore, urban disaster vulnerability (UDV) assessment is necessary in the context of typhoons. It is not only beneficial for urban resilience building but also positive for sustainability [2]. However, the current UDV of coastal cities in cyclone contexts is not yet fully satisfactory. Three issues must be addressed. Firstly, many coastal cities have attracted a large number of immigrants due to economic and other factors. This phenomenon is not slowing down at present [5], but the research on coastal high-density cities is limited. Secondly, the spatial layout and structure of the city in the urban spatial pattern are necessary for urban development [6]. In particular, the height and distribution of buildings have a significant impact on the distribution and direction of typhoon wind speed [7]. However, few studies have explored the urban spatial morphology associated with resilience in the context of typhoons. Thirdly, a notable research gap exists in the academic community

in terms of assessing the vulnerability of coastal cities to typhoons. For instance, an assessment framework and indicator system specifically for typhoon vulnerability remains unavailable. Current research focuses more on urban vulnerability. Meanwhile, assessment frameworks for typhoon vulnerability of coastal cities are neglected [6,8–11].

In response to the first research question, we believe that a UDV assessment of coastal cities characterised by high population density must be conducted at this stage given the global trend of rising population. Another reason is the continuous population flow to coastal low-elevation cities over the previous decades [1]. This condition can potentially maintain increasing population densities in coastal low-elevation cities in the future. For the second research question, computational fluid dynamics (CFD) has a huge advantage in modelling typhoon disasters in three dimensions [12,13]. However, to the best of our knowledge, only a few studies have attempted to combine this approach with UDV. We believe that a typhoon simulation using CFD is required in conjunction with urban spatial morphology to assist in UDV assessment. For the third research question, the exposure–sensitivity–adaptation model has been proposed as early as 2007 and has been accepted by many studies [14]. However, studies that utilised sufficient data across the three dimensions to fully validate the model are limited. Therefore, an assessment framework and indicator system using this model must be developed specifically for typhoon vulnerability.

Macau, a former Portuguese colony, is located in southern China, close to Hong Kong and Guangzhou. It is one of the most densely populated cities in the world [15]. In 2022, the population per square kilometre of Macau had exceeded 20,000, reaching 20,620 [16]. Macau suffers from frequent typhoon disasters due to its location in the coastal area and its subtropical climate [17]. Two of the worst typhoons in Macau's history, Hato and Mangkhut, caused severe economic losses and casualties [18]. In addition, Macau has a well-developed economy. At its peak, it ranked first in the world in terms of gross domestic product (GDP) per capita at purchasing power parity [19]. Therefore, Macau has a complex urban spatial pattern. The disaster simulation must be completed during a typhoon by using CFD. Finally, the Macau government has conducted sound statistical data disclosure, such as the age structure of the residents as fine as that of single residential buildings [16]. This condition contributes to the exposure–sensitivity–adaptation modelling. The content of the appeal reveals that the case study of Macau can provide a key reference for the construction of indicator systems for coastal cities worldwide.

2. Literature Review

In 2007, the Intergovernmental Panel on Climate Change (IPCC) report indicated that vulnerability assessment is a vital tool in addressing the challenges of climate change. The report defined vulnerability as an integrated concept composed of three dimensions: exposure, sensitivity and adaptive capacity [20], which have been widely applied [21,22]. At the urban level, especially when facing the threat of extreme weather events, conducting a comprehensive vulnerability assessment is particularly crucial. Although academic research on vulnerability assessment has progressed, many deficiencies remain and must be improved.

Firstly, a significant gap exists in current academic research regarding the vulnerability assessment and study of high-density urban areas under the impact of typhoons. Deng et al. (2020) suggested that these regions face unique challenges due to high population density, concentrated infrastructure and limited resources [23]. However, these characteristics have yet to receive adequate attention in the existing literature. Although many high-density cities are located in coastal areas, not all coastal cities exhibit the characteristics of high-density urban areas. Therefore, conducting specialised vulnerability assessments for these cities would provide new perspectives and a deeper understanding of the field. Ku et al. (2021) assessed the vulnerability of coastal areas, but their assessment lacked explicit focus on the unique requirements and challenges of high-density urban regions [24]. In the field of urban planning, methods for typhoon vulnerability assessment have been widely applied but have yet to comprehensively cover all types of cities, mainly high-density

urban areas. The risks faced by cities during typhoons stem not only from the destructive power of the typhoons themselves but also from multiple factors, such as changes in surface cover caused by urbanisation processes, inadequate drainage systems and the lack of flood defence facilities [25]. In-depth research on typhoon vulnerability in high-density urban areas becomes particularly critical to more comprehensively and accurately assess their vulnerability and susceptibility during typhoons.

Secondly, in the research on typhoon vulnerability, scholars generally focus on the impact of factors, such as climate change, population density and economic conditions [26], whereas the analysis on urban spatial forms must still be improved. Although He et al. (2017) investigated the coupling mechanism between coastal urban spatial form and mesoscale wind environment, emphasising the critical role of urban form in regulating wind environment, subsequent studies, such as that of Gao et al. (2020), did not delve into the specific impact of urban form on disaster risk when assessing the typhoon disaster risk in Zhuhai City [27,28]. Su et al. (2022) highlighted the response and recovery capabilities of urban ecosystems in typhoon disasters and the key role of urban form in reducing vulnerability. However, they failed to investigate how urban spatial layout can reduce typhoon damage, especially in terms of 3D scale analysis [29]. Current typhoon vulnerability research is often limited to considerations of 2D spatial factors, with a relative lack of in-depth analysis of urban 3D spatial form [30]. The spatial layout and structure of cities, especially the height and distribution of buildings, significantly impact the distribution and direction of wind speed. In addition, the distribution of urban green spaces regulates the urban climate and effectively slows down wind speed during typhoons, providing additional protection for the city [31]. Therefore, future research should extend to the analysis of urban 3D spatial form to more comprehensively understand its effects on typhoon vulnerability and provide more precise guidance for urban planning and disaster risk management.

Finally, in assessing the vulnerability of coastal cities to typhoons, the academic community currently faces a notable gap in research, namely, the absence of a dedicated assessment framework and indicator system for typhoon vulnerability. Jeong and Cheong (2012) and Gao et al. (2020) laid some groundwork in this area; they primarily subsume typhoon vulnerability within a broader analysis of urban-coupled vulnerability, failing to fully account for the urban spatial vulnerability factors specific to typhoon disasters [28,32]. Kim et al. (2020) attempted to develop a typhoon vulnerability function using loss records from Typhoon Maemi. However, their research should have comprehensively considered the impact of urban spatial layout and environmental characteristics [33]. Similarly, Yan et al. (2023), in exploring the spatiotemporal variations in typhoon risk in Guangdong Province, needed to provide a specialised assessment indicator and framework for typhoon vulnerability [34]. Existing research tends to incorporate typhoon vulnerability into a more general framework of urban coupled vulnerability [35–37], which often overlooks the urban spatial vulnerability factors unique to typhoon disasters. However, the impact of typhoons on cities is deeply influenced by their spatial layout and environmental characteristics [27], and thus, these specific spatial factors must be considered when assessing typhoon vulnerability. This urgently calls for the academic community to develop an assessment framework and indicator system that starts from the perspective of urban space and is aimed explicitly at typhoon vulnerability to more accurately identify and quantify the vulnerability of cities in the face of typhoon threats. To fill this research gap, future studies should focus on constructing an integrated assessment framework that includes specialised indicators for typhoon vulnerability whilst considering the 3D spatial characteristics of cities, such as the height, density and building layout, as well as the distribution of green spaces and water bodies.

In summary, despite substantial research on urban vulnerability, some academic gaps remain. The main gaps are as follows: (1) the absence of typhoon vulnerability research in high-density urban areas and (2) the insufficiency of typhoon vulnerability research, in terms of analysis and discussion, within the urban 3D space.

The present study aims to fill these gaps. Firstly, given that existing research ignored the impact of vulnerability assessment in high-density urban areas, we focus on identifying typhoon disasters and exploring adaptation strategies in high-density regions. This study conducts a spatiotemporal quantitative analysis of all typhoons that affected Macau from 2000 to 2020, investigating the spatial distribution and seasonal characteristics of typhoon disasters and revealing the main tracks of these typhoons. Moreover, line density analysis and seasonal variations are performed through GIS spatial statistics. Secondly, since 3D data can offer more details and precision than 2D data, the typhoon wind environment in Macau is numerically simulated at a 3D scale, considering the main characteristics and features of Macau's topographical surface. Thirdly, we developed an urban disaster vulnerability (UDV) assessment model using the 'exposure–sensitivity–adaptation' framework. This model aims to construct an urban disaster vulnerability assessment framework specifically for typhoon vulnerability, and a corresponding index system is established to systematically assess and quantify the vulnerability to typhoon disasters in cities. The model assesses the entire city of Macau on a grid scale to identify areas vulnerable to typhoon disasters. In addition, principal component analysis (PCA) reveals the significant factors influencing the areas prone to typhoons in Macau.

3. Material and Methods

3.1. Study Area

The Macau Special Administrative Region (SAR) of the People's Republic of China, commonly referred to as Macau, is a distinctive geographical entity situated on China's southeast coast. It is not just a pinpoint on a map, at a longitude of 113.5° east and a latitude of 22.2° north, but a region with a rich spatial diversity. Macau holds a strategic position, bordered by Zhuhai City in Guangdong Province to the north and facing Hong Kong across the Pearl River Estuary to the east (Figure 1).

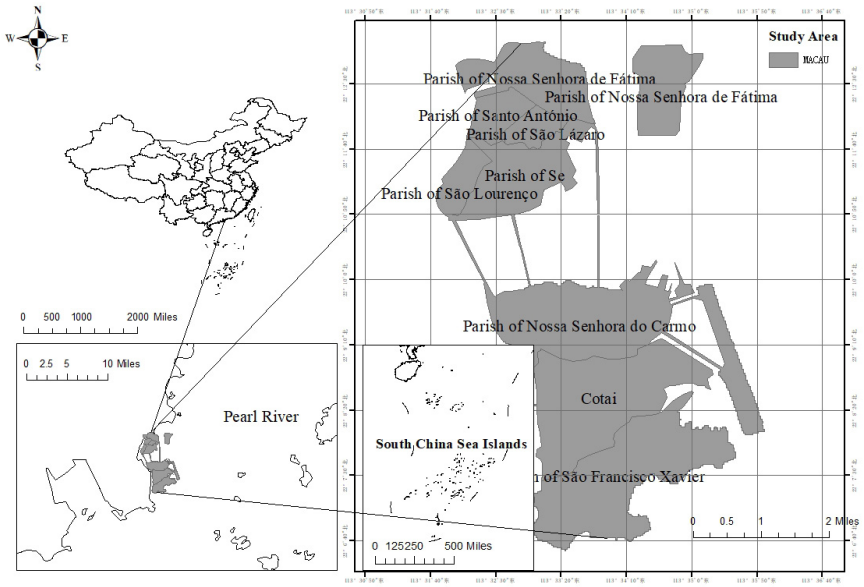


Figure 1. Location of Macau in China.

The territory of Macau is a vibrant tapestry of interconnected spaces, encompassing the Macau Peninsula, Taipa Island and Coloane Island. These areas are linked by bridges and causeways, creating a cohesive urban expanse that transcends individual points to form a unified urban landscape. This spatial configuration is visually represented in Figure 2, which illustrates the urban continuum and maritime boundaries, providing a comprehensive view of Macau's geographical layout and spatial characteristics.

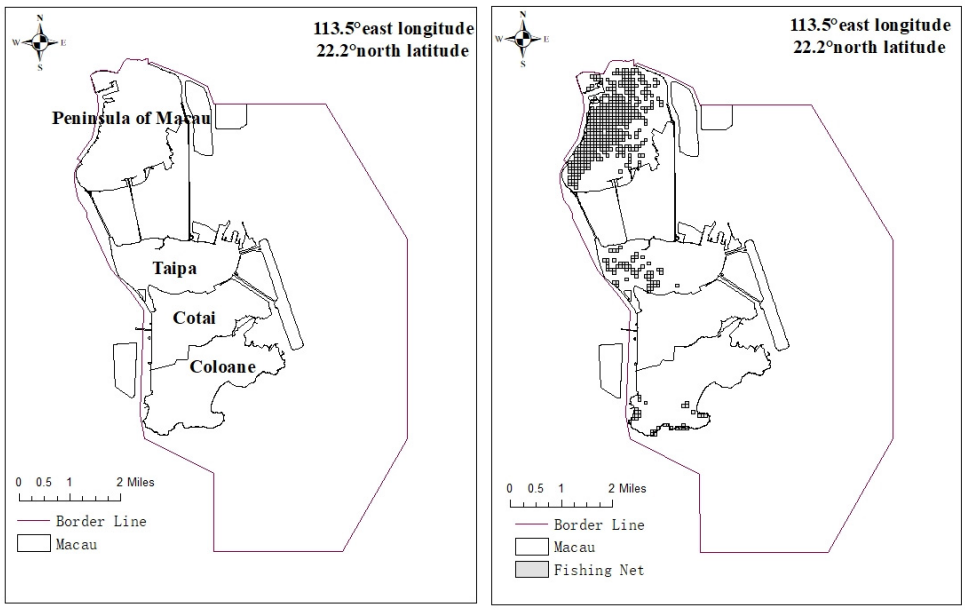


Figure 2. Macau's geographical composition and grid division.

Macau is located in the central part of the Pearl River Estuary, where tropical cyclones frequently make landfall. The meteorological disasters in Macau are mainly typhoons and rainstorms. May–November represents the season of frequent typhoons in Macau, and their activities are characterised by long duration and high frequency.

At the same time, to deeply analyse the specific situation of typhoon disasters in Macau, the method of using Macau as the base map is adopted, and detailed fishing net divisions are conducted in ArcGIS10.8.We used grids as the basic unit of analysis, eliminated invalid grids through precise data processing and finally determined the number of effective grids to be 470, which provided a solid foundation for subsequent typhoon disaster analysis (Figure 2).

3.2. Data Sources

1. CFD wind environment simulation

The wind environment simulation utilises historical typhoon data from the Macau Tropical Cyclone Record List, spanning the years 2000 to 2020. The data were extracted from the typhoon track network http://typhoon.zjwater.gov.cn/default.aspx (accessed on 17 December 2021), where we manually recorded the transit data of the listed typhoons at six-hour intervals. These data include the latitude and longitude coordinates of the typhoon centre, as well as the wind speed and pressure measurements that were obtained at the time of the typhoon's occurrence, thereby reflecting near-real-time conditions.

Currently, typhoon data is typically collected using anemometers with wind cups, tipping-bucket rain gauges, automatic weather stations, weather phenomenon instruments and CINRAD/CC-type weather radars (Table 1). In the context of these historical records, the wind pressure range for typhoons during this period was observed to be between a minimum of 895 Pa and a maximum of 1010 Pa. Wind speed, on the other hand, varied from a low of 10 km/h to a high of 72 km/h. It is important to note that wind pressure, measured in Pascals (Pa), is a physical quantity that indicates the force exerted by the wind on a unit area. A higher wind pressure suggests a stronger typhoon with greater potential for damage. Conversely, wind speed, measured in kilometres per hour (km/h), quantifies the rate at which the wind is moving. The higher the wind speed, the more intense the typhoon and the more significant the impact it can have on structures and the environment.

Table 1. Instruments and observing stations for typhoon data collection.

Equipment Name	Explanation
Anemometers with wind cups	These measure wind speed by capturing the wind's kinetic energy as it impacts the cups, which rotate at a speed proportional to the wind velocity.
Tipping-bucket rain gauges	These gauges measure rainfall by collecting rain in a bucket that tips when it fills to a certain level, providing a precise measure of precipitation.
Automatic weather stations (AWSs)	These are automated systems that measure various weather parameters, including temperature, humidity, atmospheric pressure and wind speed and direction.
Weather phenomenon instruments	These are used to observe and record various weather phenomena such as fog, thunderstorms and visibility conditions.
CINRAD/CC-type weather radars	These radar systems provide detailed information on precipitation distribution, storm movement and intensity, which are crucial for tracking and predicting typhoon paths and impacts.

2. Identification of typhoon-disaster-vulnerable areas

In the disaster assessment framework system, an increase in exposure and sensitivity increases the region's vulnerability. Thus, a positive correlation is observed amongst exposure, sensitivity and disaster vulnerability. Conversely, increasing adaptability reduces the region's vulnerability. Therefore, this article selects indicators for analysis using the framework of 'exposure–sensitivity–adaptation' combined with the literature (Figure 3).

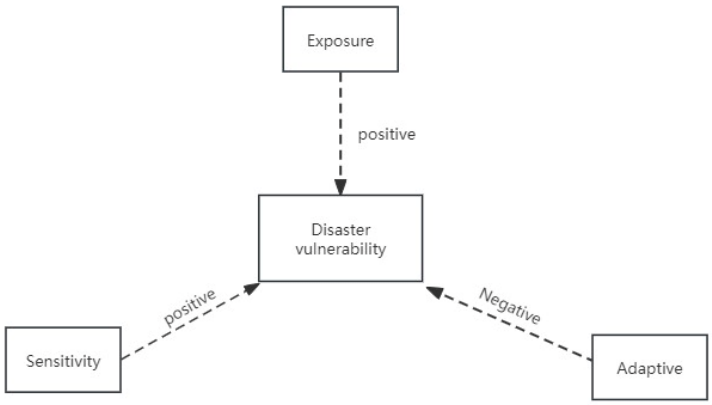


Figure 3. Disaster vulnerability assessment framework.

3. Data collection and sources

The identification of typhoon-disaster-vulnerable areas is mainly based on statistical data, spatial data and social data collection methods as follows (Table 2).

Table 2. Comprehensive calculation table of indicators.

Dimensions	Variable	Unit	Variable Calculation Specification	Correlation	Sample Size	Time Resolution	Length of Time	Number of Specific Sites	Reference	Data Source
Exposure	Building land ratio	%	Building area/unit area	+	6337	One-time survey	2021	470	[38]	Macau Cartography and Cadastre Bureau
	Wind speed	m/s	Simulation result	+	100	Every typhoon disaster	2000–2020	100	[6]	CFD simulation results
	Average elevation	m	Unit mean elevation	+	/		2021	470	[39]	Macau Cartography and Cadastre Bureau
	Population density	/km^2	Unit resident population/unit area	+	/		2022	470	[6,38,40]	World Pop 1km dataset (https://hub.worldpop.org/geodata/listing?id=76 accessed on 10 February 2022)
Sensitivity	Proportion of population over 65 years old	%	Number of people over 65 years old per unit/unit total population	+	4326	One-time survey	2011	3241	[41,42]	Macau Statistics and Census Bureau statistical geographic information system (https://www.dsec.gov.mo/gis/unidade/unidade.html?lang=cn accessed on 22 January 2022)
	Proportion of population aged 0–14	%	Number of people aged 0–14 per unit/unit total population	+						
	Proportion of female population	%	Female population per unit/total population per unit	+					[37,42]	
	Permanent resident population	Person	The number of permanent residents in a unit	+					[40,43]	
	Building age	Year	Number of years since the construction commenced	+					[44]	
Adaptability	Vegetation coverage	%	Unit green space/unit area	-	/		2022	470	[41,45]	Geographic Remote Sensing Ecological Network (http://www.gisrs.cn/infofordata?id=35bb3c58-88ce-4edb-8286-64a5e679bd33 access date 16 December 2021)
	Medical resources	/	Total number of unit medical resources	-	2145		2022	2145	[37,46]	Baidu Map

(a) Statistical data: They mainly reflect Macau's construction status and population data, which are obtained from the statistical geographic information system of the Statistics and Census Bureau of Macau.

(b) Spatial data: They describe objects to represent the shape, size, location and distribution characteristics of spatial entities, including vegetation coverage, elevation and population density. The vegetation coverage database is calculated from the 2020 Landsat image of Macau according to the vegetation coverage formula. The Cartography and Cadastre Bureau of the Macau Special Administrative Region provides elevation data. Population density data are obtained from the World Pop 1 km dataset (https://www.worldpop.org/ accessed on 10 February 2022).

(c) Social information: It mainly reflects the status of medical resources in Macau. In this article, it is represented by the points of interest (POIs) of medical resources, the source of which is Baidu Map.

3.3. Research Method

This section details the research methodology. To visually display the research design, we provide a flow chart (Figure 4) to summarise the entire research process, as follows:

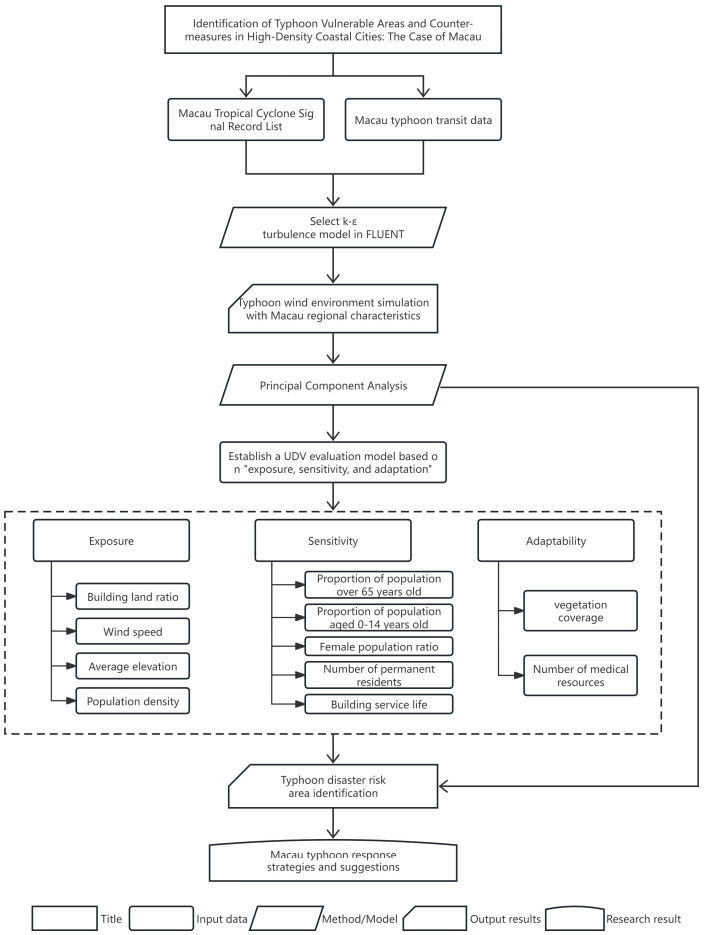


Figure 4. Research flow chart.

3.3.1. CFD Wind Environment Simulation

This article mainly studies the wind environment under severe weather caused by typhoon disasters in Macau. Thus, using field measurement and wind tunnel testing research methods is unsuitable. The CFD wind environment simulation method is used for 3D numerical simulation of the entire city of Macau. This approach aims to summarise the characteristics of the wind environment of the Macau typhoon disaster.

ANSYS FLUENT 2019 R1 is used as the simulation software for the typhoon wind ring simulation work in the Macau area. As general-purpose CFD software, FLUENT is powerful and flexible; it can be applied to various complex engineering simulations [47]. The framework equations for FLUENT simulation are as follows:

$$\frac{\partial \overline{u}_j}{\partial t} + \overline{u_j}\frac{\partial \overline{u}_j}{\partial x_j} = \frac{1}{p}\frac{\partial \overline{p}}{\partial x_i} + \frac{u}{p}\frac{\partial^2 \overline{u}_i}{\partial x_j \partial x_j} - \frac{\partial}{\partial x_j}\left(\overline{u_i u_j}\right) + \int_i \quad (1)$$

$$\frac{\partial \overline{u}_i}{\partial x_i} = 0 \quad (2)$$

$$\frac{\partial \overline{T}}{\partial t} + \overline{u_i}\frac{\partial \overline{T}}{\partial x_i} = k\frac{\partial^2 \overline{T}}{\partial X^2{}_I} \quad (3)$$

where $\overline{ui}$ represents the average speed in metres per second (m/s); ui' refers to the turbulent pulsation speed in metres per second (m/s); ρ indicates the air density in kilograms per cubic metre (kg/m^3); $\int_i$ denotes the buoyancy acceleration in metres per second squared (m/s^2); $\overline{T}$ represents the temperature, whose unit is Kelvin (K); k indicates the turbulent kinetic energy in square metres per square seconds (m^2/s^2); and ε is the turbulent energy dissipation rate in square metres per square seconds (m^2/s^2). Therefore, the k-ε model is implemented in the turbulence closure model of FLUENT simulation.

3.3.2. Principal Component Analysis

Component analysis is a statistical method that converts a group of variables that may have linear correlations into a few linearly independent variables through dimensionality reduction techniques. The set of linearly independent variables after transformation is called the principal components. The basic idea is that multiple original variables (X1, X2, . . ., Xp, m ≤ p) with a specific correlation are replaced by a set of linearly independent new comprehensive indicators (Y1, Y2, . . ., Ym). At the same time, these new comprehensive indicators reflect the information represented by the original variables to the greatest extent. Moreover, the information between the new comprehensive indicators does not overlap.

3.3.3. Vulnerable Area Identification Model Selection

Goharian et al. (2016) introduced a framework to assess the vulnerability of reservoir systems according to three factors, namely, quantified severity, potential severity and exposure. These factors were estimated using a top-down approach. The vulnerability assessment framework includes sensitivity and adaptive capacity [48]. Sensitivity, SoVI and WSACI are estimated using a bottom-up approach and formulated as follows:

The research data and process indicate that the vulnerability research applied 'exposure–sensitivity–adaptation'. Thus, the second approach is selected as the vulnerability fitting formula. As discussed in the previous literature, vulnerability is generally considered a function of exposure, sensitivity and adaptive capacity. This study adopted a commonly used model to express UDV, as follows:

$$UDV_h = \frac{Exposure(E_h) + Sensitivity(S_h) + (1 - Adaptive\ Capacity(AC_h))}{3}, \quad (4)$$

where UDV_h is the vulnerability degree of sample h, E_h is the exposure degree of sample h, S_h is the sensitivity degree of sample h and AC_h is the adaptability degree of sample h. UDV_h consists of the arithmetic mean of the exposure, sensitivity and adaptability of sample h. It is calculated by adding the three measures and dividing by 3. Each metric value is dimensionless, reflecting the comprehensive vulnerability of sample h to typhoon disasters.

4. Result

4.1. Distribution of Typhoons from 2000 to 2020

4.1.1. Spatial Distribution of Typhoons in Macau

This study provides 100 typhoon disasters that have affected Macau in the past 20 years through the list of tropical cyclone records. Moreover, relevant typhoon disasters from 2000 to 2020 are selected from the typhoon track website (http://typhoon.zjwater.gov.cn/default.aspx) (accessed on 19 January 2022). Furthermore, TXT files are used to intercept and record the latitude and longitude coordinates and wind speed. Typhoons transmit data, such as wind pressure and wind direction. Then, they are imported into ArcGIS and converted into a shapefile layer for density analysis to find the spatial law and action path of typhoon disasters affecting Macau.

The typhoon track map (Figure 5) shows that most of the typhoon tracks in the past 20 years have been relatively regular. Red cycle in the figure indicates Macau location in different administrative level (e.g. of national level). The typhoons' operating density and directional trends are summarised on the basis of the particularity and randomness of typhoon track activities. The statistics indicate that the typhoons affecting Macau in the past 20 years can be roughly divided into three different typhoon transit paths. Firstly, the trajectory of Path 1 moves from east to west, moving westward after landing in the eastern coastal area of Macau. The second path represents the track with the highest frequency of occurrence amongst the typhoon tracks affecting Macau. This path made landfall on the southeast coast of Macau and moved northwestward. According to statistics, most of them affected St. Francis Parish. Finally, the third path moves from the southern coast of Macau to the north and affects Guangdong Province and other regions.

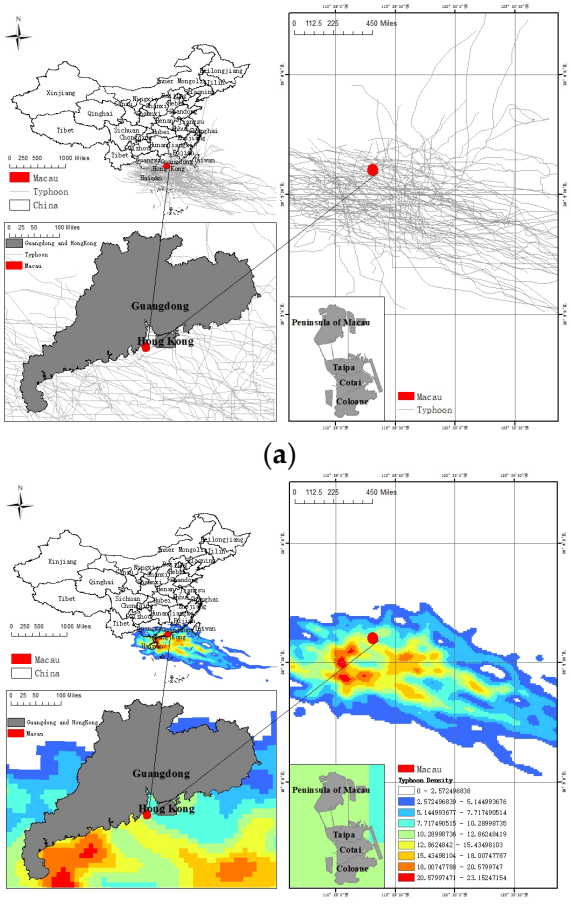


Figure 5. (**a**) Macau typhoon track pattern; (**b**) Macau typhoon density analysis and trajectory.

4.1.2. Spatio-Temporal Distribution of Typhoons in Macau

According to the investigation and research, typhoons that make landfall in or affect Macau are mainly prevalent from June to October each year and are affected by typhoon disasters, which is up to five months. Therefore, research on typhoon disasters in Macau is imminent. July to September every year represents the period when typhoons are prevalent in Macau. From 2000 to 2020, the typhoons affecting Macau in these three months accounted for 68% of the total typhoons. The data suggest that typhoon disasters in Macau have prominent seasonal characteristics. At the same time, according to the survey, August exhibits the highest frequency of typhoons. Therefore, according to the seasonal characteristics, disaster identification of typhoon disasters in Macau is considered to deal with frequent typhoon disasters in Macau.

4.2. FLUENT Wind Environment Numerical Simulation of Macau Typhoon Disasters

This study delivers a meticulous simulation encompassing the entirety of Macau's urban expanse, meticulously crafted to depict the intricacies of the wind field amidst typhoon conditions. With a strategic approach to simplifying building models, we have adeptly harmonised computational expedience with the fidelity of our simulation, thus capturing a nuanced and comprehensive depiction of Macau's urban topography.

Our simulation model underwent a stringent validation against empirical wind speed data procured from diverse locales throughout Macau (Table 3). A case in point is the Maritime Museum, where our simulation precisely predicted a wind speed of 10.45 m/s, which closely mirrors the actual recorded speed of 11.9 m/s. Further validations were conducted at key sites such as the Memorial Sun Yat-sen Park, where the simulation forecasted a wind speed of 7.496 km/h, nearly indistinguishable from the actual 7.6 km/h, and Coloane, where the simulation's 8.74 km/h was in perfect accord with the actual measurement of 8.6 km/h. At Fortress Hill, the simulation projected a wind speed of 17.49 km/h, which, while slightly above the actual 16.2 km/h, still demonstrates commendable precision (Figure 6).

Table 3. Actual wind speed at the Macau Meteorological Monitoring Station.

Number	Weather Station Monitoring Station Name	Wind Speed (km/h)
1	Dr. Sun Yat-sen Municipal Park	7.6
2	Macau Sewage Treatment Plant	19.1
3	Fortress Hill	16.2
4	Outer Harbour Ferry Terminal	23.0
5	Maritime Museum	11.9
6	East Asian Games Station	11.2
7	Macau Tai Tam Mountain	31.3
8	Coloane	8.6
9	Macau Kowloon Village	37.8
10	University of Macau	25.6
11	Sai Van Bridge	31.0
12	Governor's Bridge	34.9
13	Friendship Bridge South	42.8
14	Friendship Bridge North	40.7

Note: Data were collected from the Macau Special Administrative Region Government at 9.30 pm on 18 October 2022.

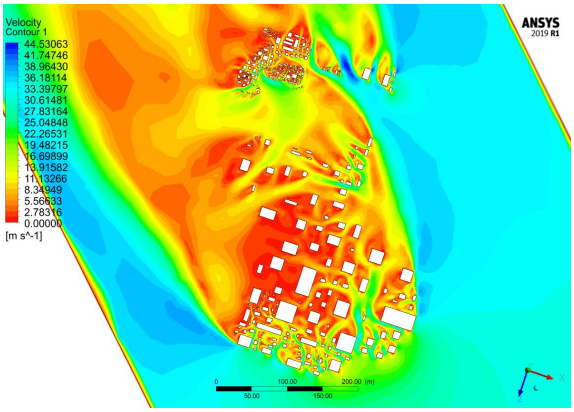


Figure 6. Simplified verification diagram of wind simulation building.

The study has meticulously examined the interaction between typhoons and Macau's unique regional features by employing simplified building data and leveraging FLUENT software. This approach has facilitated a comprehensive analysis of Macau's 3D urban wind environment and the meticulous simulation of a typhoon disaster tailored to the region's specific characteristics. The integration of these simulated wind speeds into the urban typhoon disaster vulnerability (UDV) assessment framework has notably enhanced our capacity to assess the vulnerability of Macau's districts to the devastating impacts of typhoons. The robust alignment between our simulated and actual wind speeds affirms the model's reliability in identifying areas of heightened risk from severe windstorms and their associated dangers. Furthermore, the detailed examination of Macau's 3D urban wind environment, as depicted in Figures 7–11, yields insightful and actionable intelligence. This analysis is invaluable for formulating strategic disaster preparedness measures and for guiding urban planning to effectively confront the challenges posed by typhoon threats.

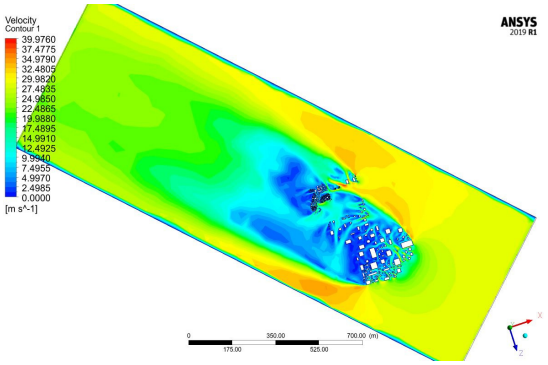


Figure 7. Simulated wind speed map of a typhoon in Macau.

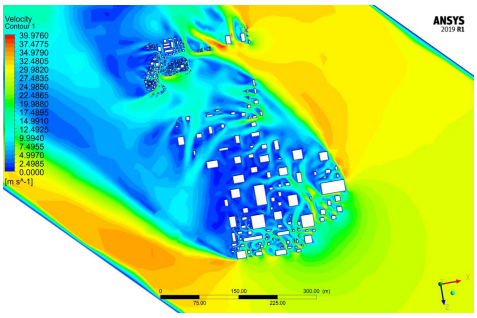


Figure 8. Partial map 1 of simulated wind speed of a typhoon in Macau.

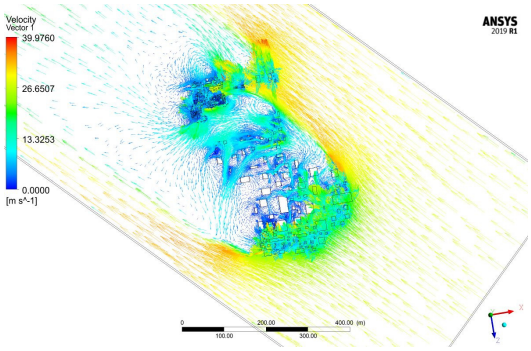


Figure 9. Partial map 2 of simulated wind speed of a typhoon in Macau.

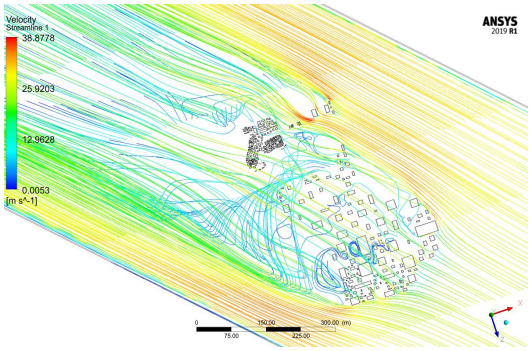


Figure 10. Partial map 3 of simulated wind speed of a typhoon in Macau.

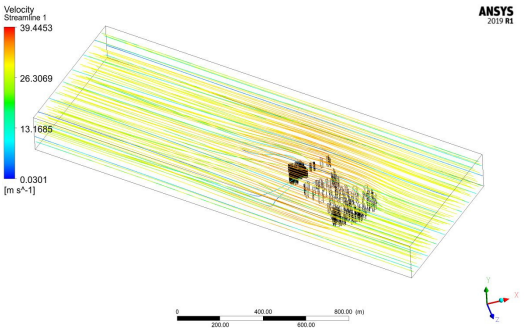


Figure 11. Panorama of simulated wind speed of a typhoon in Macau.

4.3. Numerical Simulation of a Typhoon Disaster in Macau Using FLUENT for Wind Environment

According to the evaluation model, the specific parameters of exposure, sensitivity and adaptability of 470 grids are calculated (Figure 2), and the corresponding normalised UDV values are obtained. This study further adopts the standard deviation method to objectively and reasonably discuss the statistical distribution of each category in the sample. The standard deviation category shows the difference between a feature's attribute value and the mean and the degree to which the behaviour differs from the mean. The UDV value is divided into five vulnerability levels: very low, low, medium, high and heavy.

In accordance with the evaluation of UDV in Macau, the vulnerability value and level difference are analysed. The different effects of grids on the three dimensions of UDV (exposure, sensitivity and adaptability) are highlighted by analysing the principal components. When interpreting the dimensions and principal components obtained from PCA, the criterion of 'eigenvalues greater than 1' is used. These principal components and important indicators reveal the critical indicators of the sample UDV clearly and accurately in each dimension.

4.3.1. Exposure Analysis

PCA is used for the data of four exposure indicators: the proportion of land use and buildings, wind speed, average elevation and population density (Table 4). Moreover, the two principal component solutions explain 59.43% of the variance in the dataset.

Table 4. Eigenvalues and variances of each principal component of exposure ability.

Principal Component Set	Eigenvalues	Percentage Variance	Grand Total %	Factor	Factor Loading	
					1	2
Urban development factors	1.282	32.043	32.043	Building area	0.786	0.091
				Mean elevation	0.328	0.805
				Population density	0.714	−0.046
Natural environmental factors	1.095	27.386	59.430	Average wind speed	−0.217	0.805

The first principal component includes the building footprint, average elevation and population density, integrating the current urban development and population expansion levels in Macau and therefore referred to as the urban development factors.

The second principal component comprises the average wind speed, which reflects the influence of natural disaster factors under typhoon disasters and is therefore named the natural environment factor. The exposure of Macau to typhoon disasters can be analysed more intuitively using the principal component table. Meanwhile, based on the data for each principal component, the principal component scores of 470 grids were divided into five levels using the natural-break method in ArcGIS.

These high exposures are confined to ultra-high population densities and high building footprints, resulting in a large number of residents and fewer open areas. This condition exacerbates the exposure to typhoon hazards in Macau. In addition, the average typhoon wind speed causes severe exposure of these grids, as global climate change increases likelihood of natural disasters. Macau, a high-density coastal city, is more vulnerable to typhoon hazards and more likely to cause economic losses and human casualties. Figure 12 shows that the extremely high exposure of the Chopsticks base area is caused by the high population density.

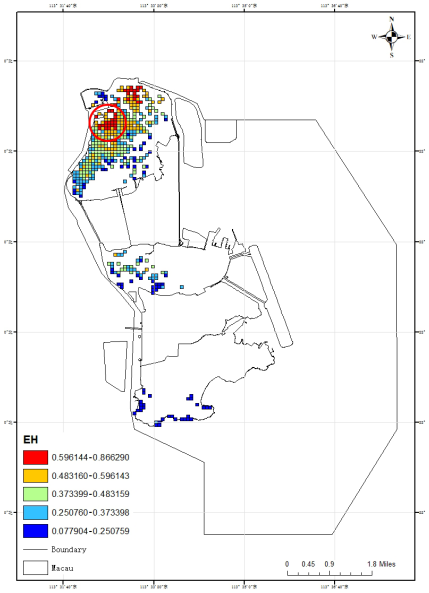


Figure 12. Spatial distribution of expositivity.

4.3.2. Sensitivity Analysis

In this study, PCA analysis was used for five sensitivity indicators: the proportion of the elderly population over 65 years old, the proportion of the female population, the proportion of the population under 14 years old, the total population and the age of buildings. In addition, the three principal components cumulatively explained 77.29% of the variance in the dataset (Table 5).

Table 5. Eigenvalues and variances of each principal component of sensitivity ability.

Principal Component Set	Eigenvalues	Percentage Variance	Grand Total %	Factor	Factor Loading
					1
Adaptability	1.017	50.871	50.871	Vegetation coverage	0.701
				Number of medical resources	0.701

The first principal component is the proportion of the elderly population over 65 years old and the proportion of the female population, collectively reflecting the current situation of vulnerable groups in Macau. The second principal component is the proportion of the population under 14 years old and the total population, reflecting the impact of the vulnerable population factor under a typhoon disaster. It is, therefore, referred to as the vulnerable population factor. The third principal component is the age of the buildings, integrally reflecting the current situation of Macau; it is termed the building factor. In accordance with the principal component table, the sensitivity of Macau to typhoon disasters is analysed more intuitively. The principal component scores of 470 grids are divided into five levels using the natural-break method in ArcGIS.

These high sensitivities are exacerbated by the high proportion of the elderly population, the proportion of the female population and the proportion of the population under 14 years old. As a result, many inhabitants are considered vulnerable, exacerbating the sensitivity of Macau to typhoon hazards. In addition, the total population is another reason for the severe exposure of these grids. The higher population size of Macau leads to a higher number of people at risk during typhoon hazards and more vulnerable to receiving typhoon hazards. Figure 13 shows that St. Anthony's Parish is extremely sensitive given the high population density within the area.

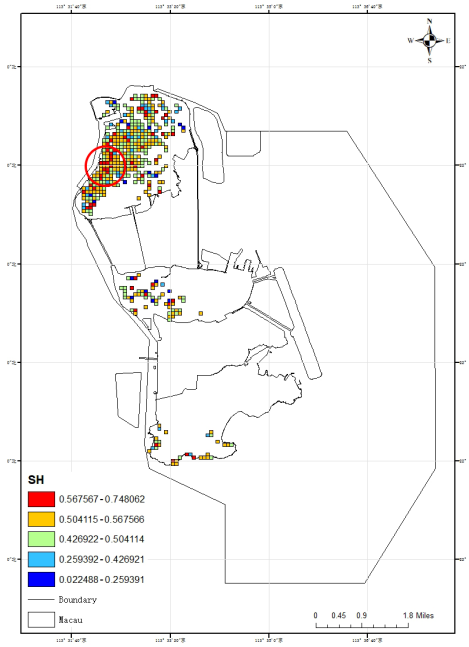


Figure 13. Spatial distribution of sensitivity.

4.3.3. Adaptive Analysis

In this study, PCA was used for two adaptation indicators: vegetation cover and number of medical resources. The principal component explained about 50.87% of the variance in the dataset (Table 6). This component contained two factors for vegetation cover and the number of medical resources. They present a factor loading of 0.701, which is higher than the minimum criterion of 0.5. Therefore, the two factors were considered suitable to remain in the theoretical model. Vegetation cover and several medical resources reflect the current adaptation status in Macau; they are referred to as the adaptation factor.

Table 6. Eigenvalues and variances of each principal component of adaptive capacity.

Principal Component Set	Eigenvalues	Percentage Variance	Grand Total %	Factor	Factor Loading		
					1	2	3
More vulnerable group factors	1.535	30.709	30.709	Proportion of the population aged 65 and over	0.773	−0.282	0.306
				Proportion of the female population	0.869	0.239	−0.136
Vulnerable population factors	1.264	25.284	55.993	Proportion of the population under the age of 14	0.367	0.729	−0.081
				Total population	−0.217	0.771	0.093
Construction factor	1.065	21.303	77.296	Building life	0.042	0.042	0.968

The vegetation cover and the number of medical resources significantly affect the improvement of adaptive capacity. Figure 14 shows that most parts of the Macau Peninsula and the coastal area of Taipa Island have excellent vegetation cover and medical resources, with high adaptive capacity.

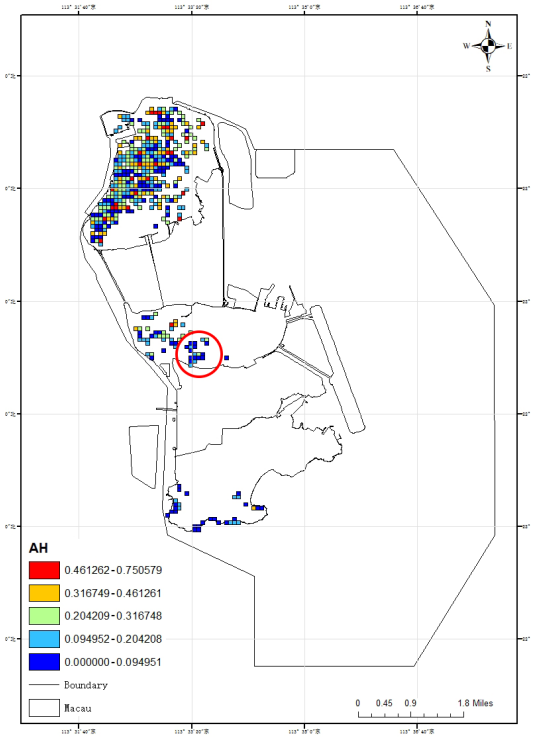


Figure 14. Spatial distribution of adaptation.

4.3.4. Analysis of UDV Vulnerability in Macau

The UDV value of vulnerability in Macau was calculated using the Moran's index. Its value was 0.155 with a z-score of 15.76, and the probability of randomly generating this clustering pattern was less than 1%. Therefore, this value exhibits spatial autocorrelation.

Meanwhile, ArcGIS is used to analyse the local autocorrelation of vulnerability UDV values in Macau and LISA regional aggregation analysis to visualise the characteristics of its spatial autocorrelation (Figure 15). The figure shows the four main types of spatial autocorrelation: high–high, low–low, high–low and low–high, as well as a blank non-significant grid. By contrast, high–low and low–high show high or low values, with spatial outliers reflecting negative local spatial autocorrelation. The figure illustrates that St. Anthony's Parish exhibits a high value of aggregation centre, indicating that the UDV value of the area requires attention and improvement. This area is undoubtedly the most vulnerable when a typhoon disaster strikes.

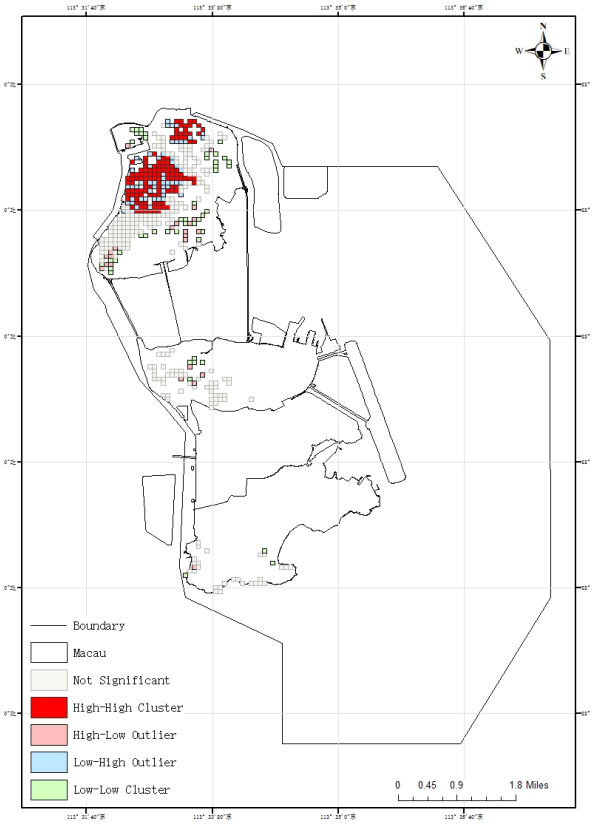


Figure 15. LISA regional aggregation map.

ArcGis 10.7 was used to calculate the mean and standard deviation of UDV values. Visualisation was conducted by highlighting the UDV values above and below the mean using the colour bands (Figure 16). In this study, the similarity statistics of exposure, sensitivity and adaptive capacity were calculated for each grid and merged into the categories closest to the squared Euclidean distance. They were defined as the Macau vulnerability UDV types: habitable, safe, generally safe, average, highly vulnerable, very vulnerable and hazardous. In addition, the two subtypes with the highest frequency in each UDV type were selected as samples. On this basis, the grid was divided into 19 subtypes to clarify the principal dimensions and components of UDV levels in different grids (Table 7).

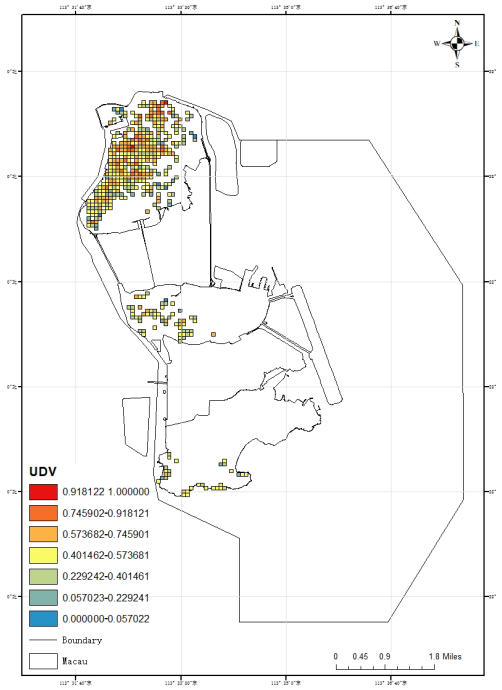


Figure 16. UDV spatial distribution.

Table 7. UDV types and levels of vulnerability, exposure, sensitivity and adaptation.

UDV Type	Serial Number	Number of Grids	Exposure	Sensitivity	Adaptability
Liveable	YJ1	1	Low	Serious	Very low
	YJ2	1	Very low	Low	Very low
	YJ3	2	Very low	High	Very low
	YJ4	1	Very low	Moderate	Low
Safe	AQ1	4	Very low	High	Very low
	AQ2	3	Very low	Moderate	Low
General security	YA1	10	Very low	High	Very low
	YA2	9	Very low	Moderate	Low
	YA3	8	Very low	Moderate	Very low
General type	YB1	11	Moderate	High	Low
	YB2	10	Moderate	Moderate	Low
	YB3	4	Moderate	Moderate	Moderate
High vulnerability	GC1	7	High	High	High
	GC2	9	High	High	Very low
	GC3	7	Moderate	High	Low
Very high vulnerability	JG1	2	High	High	Moderate
	JG2	3	High	High	Low
Dangerous	WX1	1	High	Low	Serious
	WX2	1	High	High	Moderate

Source: Author's drawing.

The liveable type has six grids, where five are divided into four subtypes. The security type has 27 grids, of which seven are divided into two subtypes. The general security type

has 105 grids, of which 27 are divided into three subtypes. The average type has 185 grids, of which 25 are divided into three subtypes. The highly vulnerable type has 118 grids, of which 23 are divided into three subtypes. The very high vulnerability type has 27 grids, of which five are divided into five subtypes. The hazardous type has two grids with two subtypes. On the basis of the main dimensions of each UDV type, the planning strategy is recommended as follows.

Habitable, safe: This grid has fewer exposure and sensitivity factors. Although the adaptive capacity is not high in this type of grid, it causes lower exposure and sensitivity. These areas are mainly characterised by high sensitivity caused by a high proportion of the elderly population, a high proportion of the female population, a high proportion of the population under 14 years old and a high proportion of vulnerable people in the total population. Urban planners should establish support organisations for vulnerable people in specific areas.

General safety type, general type: Some grids are composed of moderate exposure and sensitivity. In this grid type, exposure sensitivity is affected by some adverse factors. Theoretically, the government should adopt various urban planning measures to reduce UDV, such as controlling the expansion of construction land, reducing the building footprint and planning urban wind corridors. However, considering the actual situation of Macau as the most densely populated region in the world, the population density and buildings in large amounts cannot be controlled. Therefore, this type of planning should focus on managing land use in Macau, reducing the expansion of building sites and planning for managing illegal sites and new sites. When the plan effectively reduces exposure and sensitivity, the safe grid strategy can be used.

Highly vulnerable, extremely highly vulnerable and hazardous: Involves areas with high or very high exposure and sensitivity but low adaptability. This grid type is affected by several unfavourable factors in terms of exposure, sensitivity and adaptability. Firstly, on top of the previously mentioned control for the land use of Macau, the elevation issue must be considered. Secondly, a survey should be conducted every year prior to the typhoon season in May for buildings with high service life. A decision should be made to demolish, rebuild or reinforce the buildings according to the situation. Dangerous situations due to old buildings, such as sliding, falling off and building collapse, must be prevented. Finally, the vegetation cover must be strengthened because vegetation plays a significant role in regional typhoons. Plans to construct medical resources in the city, in a specific range, must be developed to ensure a certain number of medical institutions.

5. Conclusions

Case studies on spatial vulnerability assessment systems are common worldwide [9–11,49]. However, data from the previous literature cannot sufficiently demonstrate all the three dimensions [8,10]. In this study, the 12 cumulative indicators were completed with categorisation using three dimensions. This condition allows city managers to tailor the research results to different attributes and provides a basis for selecting indicators for future studies. Furthermore, the innovative addition of 'average wind speed' as an exposure indicator provides a critical indicator reference for future typhoon hazard vulnerability studies.

In the past, few studies have been conducted to analyse the spatial vulnerability of individual cities because another study has conducted macro- or micro-level investigations [8,9,50]. However, local governments globally tend to approach disaster policymaking from an urban perspective [51]. Therefore, this study not only filled the gaps in identifying urban wind hazard spatial vulnerability areas in Macau but also provides a reliable reference for future urban studies.

The data selected for this study are those generated from CFD simulations of typhoons in Macau. The vulnerability zones generated from these simulations are informative based on the final results. Therefore, an essential theoretical basis for whether CFD simulation data can be used to identify future wind hazard spatial vulnerability zones is provided.

In other words, with the appropriate use of CFD simulation software, the generated data are expected to be an essential data reference or supplement for identifying wind hazard spatial vulnerability zones.

Generally, the UDV evaluation index system for typhoon vulnerability in Macau is used to identify the spatial characteristics of 470 grid samples and the potential disaster vulnerability relationships in the process. A UDV evaluation pointer system is proposed to explore its principal components, and a measurement model using a series of factors is established in three dimensions: exposure, sensitivity and self-adjustment capacity. This approach aims to reveal the factors that strongly influence the typhoon vulnerability of Macau and provide targeted suggestions for future prevention and adaptation to extreme disaster weather in Macau.

The results show that 31.27% of the grid belongs to the severe vulnerable zone (SVZ) (Figure 17). UDV has six principal components with high positive and negative correlations, mainly influenced by population density, building occupancy ratio, elevation, wind speed and other indicators. Moreover, on this basis, countermeasures are proposed, as follows:

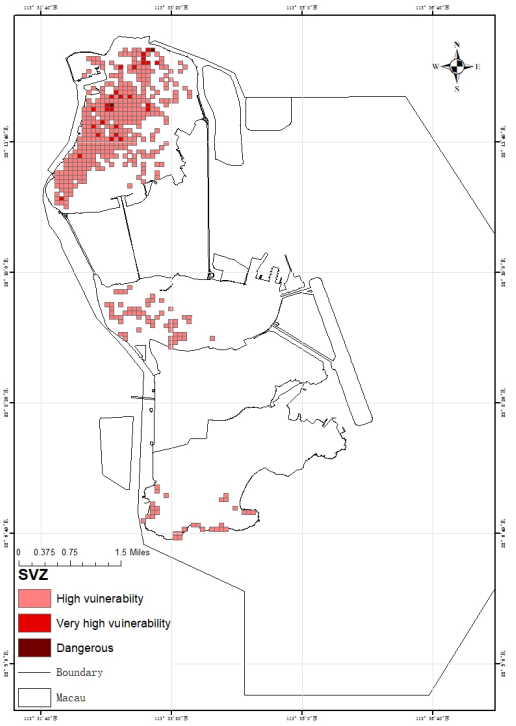


Figure 17. Severe vulnerability zone grid map.

1. Urban planners should optimise the population structure of Macau and set the building volume ratio standards in the planning and design to avoid the increase in disaster risk in this area due to the over-concentration of the population. The floor area ratio is proposed for high-rise and super-high-rise buildings based on the detailed control plans for various types of residential land prepared under the current urban planning regulation system and considering the situation in Macau. The proposed floor area ratio for high-rise buildings is 2.5–3.5, and the floor area ratio for super high-rise buildings above 19 stories is 3.6–5.
2. Support organisations must be established for disadvantaged individuals in a specific range to avoid increasing the number of injuries during typhoons.
3. A plan must be developed for controlling land use in Macau, reducing construction land expansion and managing illegal and unused land.
4. We must strengthen the vegetation cover, significantly affecting the geographical impact of typhoons. Medical resources in the city must be established in a specific range to ensure a certain number of medical institutions.

Considering the shortcomings of this study, the following research outlook is proposed: (1) The data source in this study inevitably has the problem of missing data. Therefore, pending the improvement of the database by the Macau government, future researchers can conduct another analysis on this basis to offset the inevitable experimental errors caused by missing data. (2) Future researchers can conduct specific studies on typhoon damage indicators in the direction of idle and illegal land-use planning and vegetation cover. At the same time, idle and illegal land-use planning as well as vegetation cover can be used as a single indicator to identify risky and vulnerable areas in the future, presenting a reference research path.

Author Contributions: Conceptualisation, Ziyi Chen and Long Zhou; methodology, Ziyi Chen, Long Zhou and Binglin Martin Tang; data curation, Ziyi Chen and B.M.T.; writing—original draft, Ziyi Chen and Wenrui Li; writing—review and editing, Ziyi Chen, Long Zhou, B.M.T. and Wenrui Li; validation, Wenrui Li; funding acquisition, Long Zhou; supervision, Long Zhou. All authors have read and agreed to the published version of the manuscript.

Funding: Macau Science and Technology Development Fund: 0039/2020/AFJ; National Natural Science Foundation of China: 52061160366.

Data Availability Statement: Typhoon tracks can be obtained from http://typhoon.zjwater.gov.cn/default.aspx (accessed on 19 January 2022), population density data can be obtained from https://www.worldpop.org/ (accessed on 10 February 2022) and population data and building data can be obtained from https://www.dsec.gov.mo/gis/unidade/unidade.html?lang=cn (accessed on 22 January 2022).

Conflicts of Interest: The research was conducted in the absence of any commercial or financial relationships that could be construed as a potential conflict of interest.

References

1. Neumann, B.; Vafeidis, A.T.; Zimmermann, J.; Nicholls, R.J. Future coastal population growth and exposure to sea-level rise and coastal flooding—A global assessment. *PLoS ONE* **2015**, *10*, e0118571. [CrossRef] [PubMed]
2. Lei, Y.; Liu, C.; Zhang, L.; Wan, J.; Li, D.; Yue, Q.; Guo, Y. Adaptive governance to typhoon disasters for coastal sustainability: A case study in Guangdong, China. *Environ. Sci. Policy* **2015**, *54*, 281–286. [CrossRef]
3. Shultz, J.M.; Kossin, J.P.; Ali, A.; Borowy, V.; Fugate, C.; Espinel, Z.; Galea, S. Superimposed threats to population health from tropical cyclones in the prevaccine era of COVID-19. *Lancet Planet. Health* **2020**, *4*, e506–e508. [CrossRef] [PubMed]
4. Mukherjee, A.B.; Bardhan, S. Flood vulnerability and slum concentration mapping in the Indian city of Kolkata: A post-Amphan analysis. *Water Sci.* **2021**, *35*, 109–126. [CrossRef]
5. Eadie, P. Typhoon Yolanda and post-disaster resilience: Problems and challenges. *Asia Pac. Viewp.* **2019**, *60*, 94–107. [CrossRef]
6. Nguyen, K.-A.; Liou, Y.-A.; Vo, T.-H.; Cham, D.D.; Nguyen, H.S. Evaluation of urban greenspace vulnerability to typhoon in Taiwan. *Urban For. Urban Green.* **2021**, *63*, 127191. [CrossRef]
7. ShultzLi, Q.S.; He, J.Y.; Zhou, K.; Li, X.; Chan, P.W.; Li, L. City-Scale Typhoon Hazard Analysis and Field Monitoring of Wind Effects on Skyscrapers during Super Typhoon Mangkhut. *J. Struct. Eng.* **2022**, *148*, 04022008. [CrossRef]
8. Shepard, C.C.; Agostini, V.N.; Gilmer, B.; Allen, T.; Stone, J.; Brooks, W.; Beck, M.W. Assessing future risk: Quantifying the effects of sea level rise on storm surge risk for the southern shores of Long Island, New York. *Nat. Hazards* **2012**, *60*, 727–745. [CrossRef]
9. Yu, T.; Leng, H.; Yuan, Q.; Jiang, C. Vulnerability Evaluation of Villages Based on Social–Ecological Indicators and Strategies for Improvement: Case Study of Villages in the Northeast China Plain. *J. Urban Plan. Dev.* **2022**, *148*, 04021059. [CrossRef]
10. Dewan, A.M. Vulnerability and risk assessment. In *Floods in a Megacity*; Springer: Berlin/Heidelberg, Germany, 2013; pp. 139–177.
11. Weis, S.W.M.; Agostini, V.N.; Roth, L.M.; Gilmer, B.; Schill, S.R.; Knowles, J.E.; Blyther, R. Assessing vulnerability: An integrated approach for mapping adaptive capacity, sensitivity, and exposure. *Clim. Chang.* **2016**, *136*, 615–629. [CrossRef]
12. Pantua, C.A.J.; Calautit, J.K.; Wu, Y. A fluid-structure interaction (FSI) and energy generation modelling for roof mounted renewable energy installations in buildings for extreme weather and typhoon resilience. *Renew. Energy* **2020**, *160*, 770–787. [CrossRef]
13. Yang, Y.; Dong, L.; Li, J.; Li, W.; Sheng, D.; Zhang, H. A refined model of a typhoon near-surface wind field based on CFD. *Nat. Hazards* **2022**, *114*, 389–404. [CrossRef]
14. Pachauri, R.K.; Reisinger, A. IPCC fourth assessment report. *IPCC Geneva* **2007**, *2007*, 044023.
15. Wikiwand—List of Cities Proper by Population Density. Wikiwand. Available online: https://www.wikiwand.com/en/List_of_cities_proper_by_population_density (accessed on 19 March 2024).
16. Resultados Globais dos Censos 2021 (Direcção dos Serviços de Estatística e Censos). Available online: https://www.gsef.gov.mo/pt/posts/5798 (accessed on 19 March 2024).

17. Lau, Y.; Chau, K.Y.; Dulebenets, M.A.; Tang, Y.M.; Guan, J.; Ying, T.K. Tropical Cyclone Research in Asia: Hong Kong and Macau. In *IOP Conference Series: Earth and Environmental Science*; IOP Publishing: Bristol, UK, 2021.
18. Takagi, H.; Yi, X.; Fan, J. Public perception of typhoon signals and response in Macau: Did disaster response improve between the 2017 Hato and 2018 Mangkhut typhoons? Georisk Assess. *Manag. Risk Eng. Syst. Geohazards* **2021**, *15*, 76–82. [CrossRef]
19. O'Regan, M. Post-Colonial Macau: Hope and despair in a World Centre of Tourism and Leisure. *Via Tour. Rev.* **2019**, *16*, 1–17. [CrossRef]
20. Parry, M.L.; Canziani, O.; Palutikof, J.; Van der Linden, P.; Hanson, C. *Climate Change 2007—Impacts, Adaptation and Vulnerability: Working Group II Contribution to the Fourth Assessment Report of the IPCC*; Cambridge University Press: Cambridge, UK, 2007; Volume 4.
21. De Sherbinin, A.; Bukvic, A.; Rohat, G.; Gall, M.; McCusker, B.; Preston, B.; Apotsos, A.; Fish, C.; Kienberger, S.; Muhonda, P.; et al. Climate vulnerability mapping: A systematic review and future prospects. *WIREs Clim. Chang.* **2019**, *10*, e600. [CrossRef]
22. Estoque, R.C.; Ooba, M.; Seposo, X.T.; Togawa, T.; Hijioka, Y.; Takahashi, K.; Nakamura, S. Heat health risk assessment in Philippine cities using remotely sensed data and social-ecological indicators. *Nat. Commun.* **2020**, *11*, 1581. [CrossRef] [PubMed]
23. Deng, J.; Fang, S.; Lin, X.; Cai, P. Risk Analysis and Protection Strategy of Coastal Urban Construction Project under Extreme Typhoon Climate–A Case Study of Xiamen City. *IOP Conf. Ser. Earth Environ. Sci.* **2020**, *510*, 062002. [CrossRef]
24. Ku, H.; Kim, T.; Song, Y. Coastal vulnerability assessment of sea-level rise associated with typhoon-induced surges in South Korea. *Ocean Coast. Manag.* **2021**, *213*, 105884. [CrossRef]
25. Pathak, S.; Liu, M.; Jato-Espino, D.; Zevenbergen, C. Social, economic and environmental assessment of urban sub-catchment flood risks using a multi-criteria approach: A case study in Mumbai City, India. *J. Hydrol.* **2020**, *591*, 125216. [CrossRef]
26. Hallegatte, S. A framework to investigate the economic growth impact of sea level rise. *Environ. Res. Lett.* **2012**, *7*, 015604. [CrossRef]
27. He, K.; Han, X.; He, Y.; Zhao, C. Study on the Coupling Mechanism of Urban Spatial form in Coastal City and Mesoscale Wind Environment Based on Multi-variable Analysis-Study Significance, Content, Targets and Innovation Points. In *2017 Global Conference on Mechanics and Civil Engineering (GCMCE 2017)*; Atlantis Press: Amsterdam, The Netherlands, 2017; pp. 305–309. [CrossRef]
28. Gao, Z.; Wan, R.; Ye, Q.; Fan, W.; Guo, S.; Ulgiati, S.; Dong, X. Typhoon Disaster Risk Assessment Based on Emergy Theory: A Case Study of Zhuhai City, Guangdong Province, China. *Sustainability* **2020**, *12*, 4212. [CrossRef]
29. Su, M.; Wu, J.; Feng, M. Responses of Urban Ecosystem Vulnerability and Restoration Assessment on Typhoon Disaster: A Case Study of Zhuhai City, China. *J. Sens.* **2022**, *2022*, e8344619. [CrossRef]
30. Resio, D.T.; Westerink, J.J. Modeling the physics of storm surges. *Phys. Today* **2008**, *61*, 33–38. [CrossRef]
31. Chen, W.Y.; Jim, C.Y. Resident valuation and expectation of the urban greening project in Zhuhai, China. *J. Environ. Plan. Manag.* **2011**, *54*, 851–869. [CrossRef]
32. Jeong, S.; Cheong, T. Web GIS Based Typhoon Committee Disaster Information System for Typhoon Disaster Risk Management. *Trop. Cyclone Res. Rev.* **2012**, *1*, 207–212. [CrossRef]
33. Kim, J.-M.; Son, K.; Yum, S.-G.; Ahn, S.; Ferreira, T. Typhoon vulnerability analysis in South Korea utilizing damage record of typhoon Maemi. *Adv. Civ. Eng.* **2020**, *2020*, 8885916. [CrossRef]
34. Yan, L.; He, L.; Liu, B.; Zhang, C.; Luo, H.; Tian, Z. Research on Typhoon Risk of Spatial and Temporal Differences in Guangdong Province. In Proceedings of the IGARSS 2023—2023 IEEE International Geoscience and Remote Sensing Symposium, Pasadena, CA, USA, 16–21 July 2023; pp. 2528–2531. Available online: https://ieeexplore.ieee.org/abstract/document/10283289/ (accessed on 1 May 2024).
35. Nasiri, H.; Mohd Yusof, M.J.; Mohammad Ali, T.A. An overview to flood vulnerability assessment methods. *Sustain. Water Resour. Manag.* **2016**, *2*, 331–336. [CrossRef]
36. Papathoma, M.; Dominey-Howes, D. Tsunami vulnerability assessment and its implications for coastal hazard analysis and disaster management planning, Gulf of Corinth, Greece. *Nat. Hazards Earth Syst. Sci.* **2003**, *3*, 733–747. [CrossRef]
37. Zhang, Y.; Fan, G.; He, Y.; Cao, L. Risk assessment of typhoon disaster for the Yangtze River Delta of China. *Geomat. Nat. Hazards Risk* **2017**, *8*, 1580–1591. [CrossRef]
38. Apreda, C.; D'Ambrosio, V.; Di Martino, F. A climate vulnerability and impact assessment model for complex urban systems. *Environ. Sci. Policy* **2019**, *93*, 11–26. [CrossRef]
39. Wang, P.; Liu, Z.; Zhang, L. Sustainability of compact cities: A review of Inter-Building Effect on building energy and solar energy use. *Sustain. Cities Soc.* **2021**, *72*, 103035. [CrossRef]
40. Stolte, T.R.; Koks, E.E.; de Moel, H.; Reimann, L.; van Vliet, J.; de Ruiter, M.C.; Ward, P.J. VulneraCity—Drivers and dynamics of urban vulnerability based on a global systematic literature review. *Int. J. Disaster Risk Reduct.* **2024**, *108*, 104535. [CrossRef]
41. Karimi, M.; Nazari, R.; Dutova, D.; Khanbilvardi, R.; Ghandehari, M. A conceptual framework for environmental risk and social vulnerability assessment in complex urban settings. *Urban Clim.* **2018**, *26*, 161–173. [CrossRef]
42. Müller, A.; Reiter, J.; Weiland, U. Assessment of urban vulnerability towards floods using an indicator-based approach—A case study for Santiago de Chile. *Nat. Hazards Earth Syst. Sci.* **2011**, *11*, 2107–2123. [CrossRef]
43. Song, J.; Chang, Z.; Li, W.; Feng, Z.; Wu, J.; Cao, Q.; Liu, J. Resilience-vulnerability balance to urban flooding: A case study in a densely populated coastal city in China. *Cities* **2019**, *95*, 102381. [CrossRef]

44. Rana, I.A.; Routray, J.K. Multidimensional Model for Vulnerability Assessment of Urban Flooding: An Empirical Study in Pakistan. *Int. J. Disaster Risk Sci.* **2018**, *9*, 359–375. [CrossRef]
45. Yang, X.; Liu, S.; Jia, C.; Liu, Y.; Yu, C. Vulnerability assessment and management planning for the ecological environment in urban wetlands. *J. Environ. Manag.* **2021**, *298*, 113540. [CrossRef] [PubMed]
46. Liu, J.; Gong, J.-H.; Liang, J.-M.; Li, Y.; Kang, L.-C.; Song, L.-L.; Shi, S.-X. A quantitative method for storm surge vulnerability assessment—A case study of Weihai city. *Int. J. Digit. Earth* **2017**, *10*, 539–559. [CrossRef]
47. Guide, A.F.T. *Ansys Fluent Tutorial Guide*; Ansys Inc.: Beltsville, MD, USA, 2013; Volume 15.
48. Goharian, E.; Burian, S.J.; Bardsley, T.; Strong, C. Incorporating potential severity into vulnerability assessment of water supply systems under climate change conditions. *J. Water Resour. Plan. Manag.* **2016**, *142*, 04015051. [CrossRef]
49. Nguyen, K.-A.; Liou, Y.-A.; Terry, J.P. Vulnerability of Vietnam to typhoons: A spatial assessment based on hazards, exposure and adaptive capacity. *Sci. Total Environ.* **2019**, *682*, 31–46. [CrossRef] [PubMed]
50. Chen, S.; Zha, X.; Bai, Y.; Wang, L. Evaluation of soil erosion vulnerability on the basis of exposure, sensitivity, and adaptive capacity: A case study in the Zhuxi watershed, Changting, Fujian Province, Southern China. *Catena* **2019**, *177*, 57–69. [CrossRef]
51. Garschagen, M. Decentralizing urban disaster risk management in a centralized system? Agendas, actors and contentions in Vietnam. *Habitat Int.* **2016**, *52*, 43–49. [CrossRef]

Disclaimer/Publisher's Note: The statements, opinions and data contained in all publications are solely those of the individual author(s) and contributor(s) and not of MDPI and/or the editor(s). MDPI and/or the editor(s) disclaim responsibility for any injury to people or property resulting from any ideas, methods, instructions or products referred to in the content.